Proceedings of ASME Turbo Expo 2002
June 3-6, 2002
Amsterdam, The Netherlands

2002-GT-30559

INLET FOGGING OF GAS TURBINE ENGINES: CLIMATIC ANALYSIS OF GAS TURBINE EVAPORATIVE COOLING POTENTIAL OF INTERNATIONAL LOCATIONS

Mustapha Chaker, Ph.D.
Cyrus B. Meher-Homji
Mee Industries Inc., Gas Turbine Division
Monrovia, California

ABSTRACT

Inlet fogging of gas turbine engines has attained considerable popularity due to the ease of installation and the relatively low first cost compared to other inlet cooling methods. With increasing demand for power and with shortages envisioned especially during the peak load times during the summers, there is a need to boost gas turbine power. There is a sizable evaporative cooling potential throughout the world when the climatic data is evaluated based on an analysis of *coincident wet bulb and dry bulb information*. This data is not readily available to plant users. In this paper, a detailed climatic analysis is made of 106 major locations over the world to provide the hours of cooling that can be obtained by direct evaporative cooling. This data will allow gas turbine operators to easily make an assessment of the economics of evaporative fogging. The paper also covers an introduction to direct evaporative cooling and the methodology and data analysis used to derive the cooling potential. Simulation runs have been made for gas turbine simple cycles showing effects of fogging for a GE Frame 7EA and a GE Frame 9FA Gas turbine for 60 and 50 Hz applications.

NOMENCLATURE

ASHRE	American Society of Heating and Refrigeration Engineers
CCPP	Combined Cycle Power Plant
DB	Dry Bulb Temp, °C
ECDH	Equivalent Cooling Degree Hours, °C hrs (°F hrs)
EPC	Engineering Procurement and Construction
HRSG	Heat Recovery Steam Generator
GPM	Gallons/minute
LPM	Liters/minute
NP	Net Power
WB	Wet Bulb Temp, °C
WBD	Wet Bulb Depression, °C
MWB	Minimum Wet Bulb Temp, °C
WG	Water Gauge

1. INTRODUCTION

Gas Turbine output is a strong function of the ambient air temperature with power output dropping by 0.54-0.9% for every 1°C rise in ambient temperature (0.3-0.5 % per 1°F). On several heavy frame gas turbines, power output drops of around 20% can be experienced when ambient temperatures reach 35°C (95°F), coupled with a heat rate increase of about 5%. Aeroderivative gas turbines exhibit even a greater sensitivity to ambient conditions. A representation of the power boost capability for given inlet cooling potential for different types of gas turbines is shown in Figure 1. This was derived using GTPRO[1] software over a range of turbines.

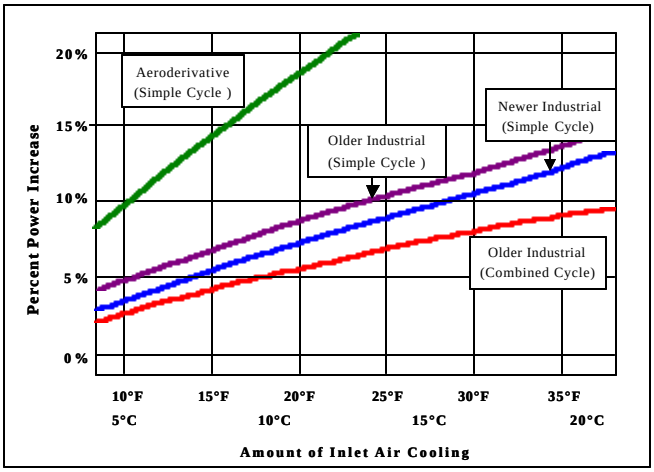

Figure 1. Representation of power boost possible by inlet cooling.

This loss in output presents a significant problem to utilities, cogenerators and independent power producers when electric demands are high during hot summer months. In the petrochemical and process industries, the reduction in output of mechanical drive gas turbines often curtails plant output. For example, at some

[1] Program by Thermoflow Inc.

liquefied natural gas (LNG) plants, production may have to be curtailed during the hot afternoons when the refrigeration capacity is limited by gas turbine driver power. One way to counter this drop is to cool the inlet air. While there are several cooling technologies available, fogging has seen large-scale application because of the advantage of low first cost when compared to other techniques including media evaporative cooling and refrigeration technologies[2]. Chaker et al [1] has provided a detailed analysis of the evaporative cooling potential in terms of Equivalent Degree Cooling Hours (ECDH) for a large number of sites in the USA. In this paper the same methodology is extended for 106 international locations outside the United States.

A major obstacle faced by gas turbine users in analyzing the potential for fog evaporative cooling is that there is sparse climatic data available *in a form that users can make a decision on the benefits of evaporative cooling*. The obstacle may be broken into two factors:

(1)] Operators cannot easily locate the appropriate weather data for their site. Much of the data is available at a plant site may be based on *average* data points with no representation of the values of *coincident* dry and wet bulb temperatures. This data is invaluable when evaluating any evaporative cooling solution.

(2) Even when some appropriate data is available through web sites or other sources, the data tables and information are not in a format to enables an operator to rapidly access the potential of evaporative cooling. The data has to be considerably massaged and collated before a meaningful estimate can be made of cooling potential at the site.

The object of this paper is to provide an easy to use solution to this problem providing a detailed analysis of multiple locations all over the world to allow users to evaluate power augmentation potential. This paper is intended to allow a rapid evaluation of site-specific cooling potential. McNeilly [2] has provided an excellent study on the importance of accurate climatic data when evaluating gas turbine inlet cooling projects. The relative potential of different gas turbines to capacity increase due to inlet cooling has been evaluated by Kitchen et al [3].

In order to keep this paper self contained, some of the basic concepts of fog evaporative cooling are presented below.

2. OVERVIEW OF POWER AUGMENTATION STRATEGIES

There are several power augmentation strategies for gas turbines. These include:

- Gas turbine inlet refrigeration- utilizing absorption or mechanical refrigeration
- Inlet fogging
- HRSG supplemental firing -applies to Combined Cycle Power Plants (CCPP) only.
- Gas turbine water/steam injection

A detailed study conducted by Tawney et al [4] evaluated several options for power augmentation for combined cycle power plants. The results indicated that the option with the minimal EPC cost impact was inlet fogging. Inlet fogging was the only option that provided a small augmentation in heat rate, while the other options all worsened heat rate. In terms of return on equity, the highest return on investment was obtained by the combination of inlet fogging and supplemental firing of the HRSG. As a practical matter, several CCPPs are adopting fogging as a power augmentation strategy. This trend is being noted not only in the USA but in several parts of the world. Jones and Jacobs [5] have also studied various power enhancement techniques of combined cycle power plants.

3. OVERVIEW OF EVAPORATIVE COOLING TECHNOLOGIES

3.1 Traditional Media Based Evaporative Cooling Technology

Traditional media based evaporative coolers have been widely used in the gas turbine industry especially in hot arid areas. The basic principle of evaporative cooling is that as water evaporates, it cools the air because of the latent heat of vaporization.

Traditional Evaporative Coolers are described in detail by Johnson, [6].

Evaporative cooler effectiveness is given by:

$$E = \frac{T_{1DB} - T_{2DB}}{T_{1DB} - T_{2WB}} \qquad (1)$$

Where,

T_1 = inlet temperature
T_2 = exit temperature of evaporative cooler
DB = dry bulb
WB = wet bulb

A typical value for effectiveness is 85-90%, which implies that the wet bulb temperature can never be attained.

The temperature drop assuming an effectiveness of 0.9, is given by:

$$\Delta T_{DB} = 0.9\left(T_{1DB} - T_{2WB}\right) \qquad (2)$$

A psychometric chart can be used to obtain the value of the WBT. The exact power increase depends on the particular machine type, site altitude and ambient conditions.

The presence of a media type evaporative cooler inherently creates a pressure drop that results in a drop in turbine output. As a rough rule of thumb, a 1" WG (2.54 cm WG) increase in inlet duct losses will result in a 0.35-0.48% drop in power and a 0.12% increase in heat rate. These numbers would be somewhat higher for an aeroderivative machine. The key issue with a traditional media evaporative cooler is that this increased pressure drop loss occurs year round even when the evaporative cooler is not in use. Increases in inlet duct differential pressure will cause a reduction of compressor mass flow and engine operating pressure. Increase in inlet differential pressure results in a reduction of the turbine expansion ratio.

The inherent loss of efficiency and increased inlet pressure loss in a traditional evaporative cooling system never allows for the maximum cooling effect to be attained. Water quality requirements are, however, less stringent than those required for direct fog cooling systems.

3.2 Inlet Fogging Technology

Direct inlet fogging is a method of cooling where demineralized water is converted into a fog by means of special atomizing nozzles operating at 138 Bar (2000 psi). Details pertaining to the thermodynamics and practical aspects of fogging have been described

[2] Cost ratios are about 5:1 but can vary based on project specifics.

in Meher-Homji and Mee [7,8]. The fog provides cooling when it evaporates in the air inlet duct of the gas turbine. This technique allows close to 100% effectiveness in terms of attaining 100 percent relative humidity at the gas turbine inlet and thereby gives the lowest temperature possible (the wet bulb temperature) without refrigeration. Direct high pressure inlet fogging can also be used to create a compressor intercooling effect by allowing excess fog into the compressor, thus boosting the power output considerably. In this paper, consideration is only made of *evaporative* fogging alone, with no discussion of fog intercooling being considered. A detailed parametric analysis of gas turbine response to fogging has been provided by Bhargava and Meher-Homji [9]. An application of fog intercooling on heavy-duty gas turbines is described by Ingistov [10]. A photograph showing a typical high pressure fogging skid is shown in Figure 2.

Figure 2. Typical high pressure fogging skid. The feed lines from the high pressure pumps to the inlet system can be seen here.

Inlet fogging includes a series of high pressure reciprocating pumps providing demineralized water to an array of fogging nozzles located after the air filter elements. The nozzles create a large number of micron size droplets which evaporate cooling the inlet air to wet bulb conditions. A photo of a nozzle array fogging an inlet duct for a large frame gas turbine is shown in Figure 3. A typical fog plume emanating from a single nozzle is shown in Figure 4.

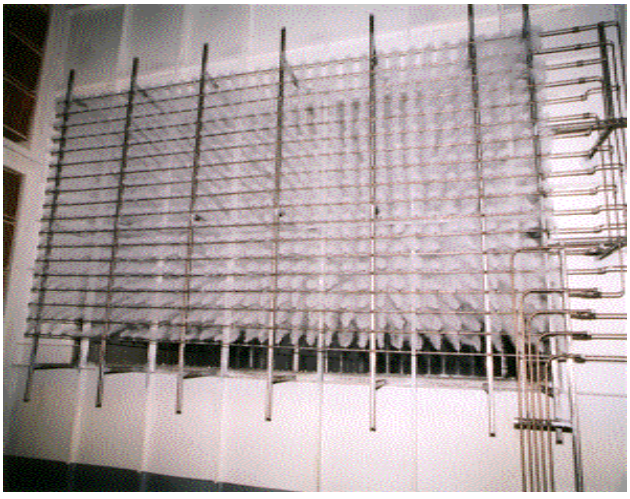

Figure 3. High pressure fogging skid in operation for a heavy-duty gas turbine.

Figure 4. Typical fog plume from a single fog nozzle.

4. CLIMATIC AND PSYCHROMETRIC ASPECTS OF INLET FOGGING

4.1 Control of Inlet Fogging Systems and the Importance of Climatic Data.

The control system of most inlet fogging systems incorporates a programmable logic controller (PLC), which is mounted on the high-pressure pump skid. Sensors are provided to measure ambient relative humidity and dry bulb temperature. Programming algorithms within the PLC use these measured parameters to compute the ambient wet bulb temperature and the wet bulb depression (i.e., the difference between the dry bulb and wet bulb temperature) to quantify and control the amount of evaporative cooling that is possible at the prevailing ambient conditions. The system turns on (or off) fog cooling stages to match the ability of the ambient air conditions to absorb water vapor. The software would then be configured to adjust the amount of fog injected in proportion to the inlet air mass flow.

By choosing pump displacements (i.e., flow in gpm) it is possible to derive multiple cooling stages with the utilization of different pump combinations.

Obviously, the control of the skid is based on climatic conditions and so the overall utilization of the fogging system at any location, is a strong function of the climatic conditions. It is this reason that makes an accurate understanding of the variations in climatic conditions an imperative. McNeilly, [2] has addressed the area of climatic data for evaporative cooling.

4.2 Modeling of Climatic Data

There are numerous problems and traps when modeling climatic data- several of which derive from the concept of "averaging" of data. One example of this is using data such as shown in Figure 5. This figure provides a correlation of dry bulb and wet bulb averages at a certain site. The graph shows that the linear behavior may lead one to conclude that at a dry bulb temperature of 25°C, the expected wet bulb is 20°C allowing a wet bulb depression of 5°C. (i.e., a measure of evaporative cooling potential). This is totally erroneous as the data was derived by taking the *average* WB temperature and the *average* DB temperature and plotting the curve. Consequently, the graph does *not* reflect *coincident* WB and DB conditions and will

therefore indicate a much reduced cooling potential. It is advisable that the site's temperature profile for a full year of hourly data with the 20-30 year average wet and dry bulb coincident temperatures be considered in the analysis. These data can be used to generate "evaporative cooling degree hour" (ECDH) numbers for each hour of the year and allow a turbine operator to make a very detailed and accurate analysis of potential power gain from inlet fogging.

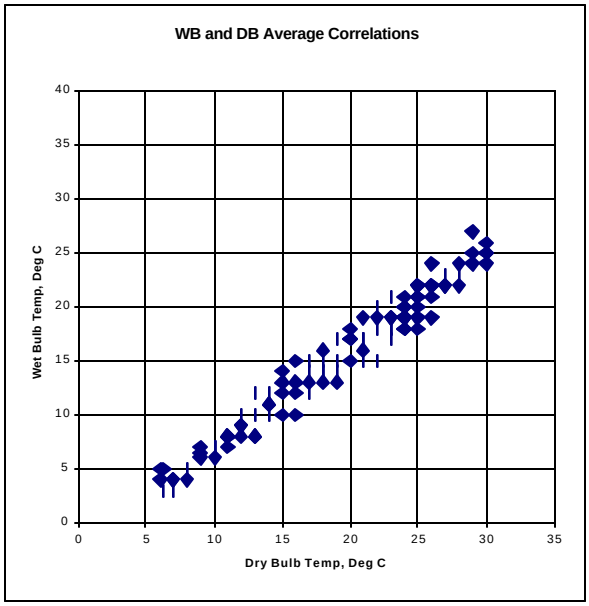

Figure 5. Correlation of WB and DB temperatures - averaged data.

High relative humidity conditions do not occur with high dry bulb temperatures. A typical pattern of variation of dry bulb and wet bulb temperature over a day is depicted in Figure 6. As can be seen, during the afternoon hours, there is a considerable difference between the wet bulb and dry bulb temperatures. It is this spread that allows the use of fog evaporative cooling.

A common mistake made by users is to take the reported high relative humidity and temperature for a given month and base the design on these. The problem is that the high relative humidity generally occurs time-coincident with the lowest temperature and the lowest relative humidity occurs with the highest temperature. This mistake results in the erroneous conclusion that very little evaporative cooling can be accomplished and has historically been the underlying cause of the maxim that evaporative cooling is not possible in "high humidity regions".

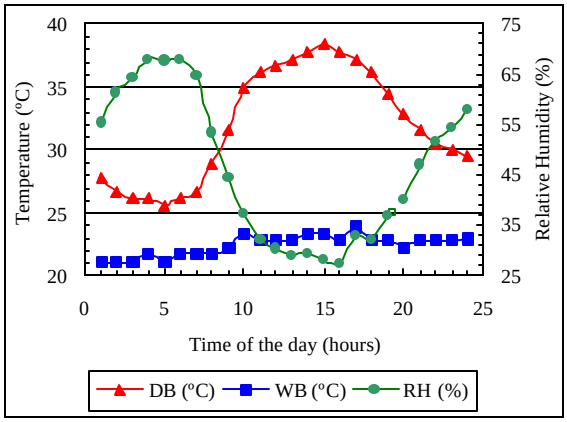

Figure 6. Daily variation of dry bulb and wet bulb temperatures.

4.3 Fog Evaporative Cooling in High Humidity Regions.

Even the most humid environments allow for up to 8°C (15°F) of evaporative cooling during the hotter part of the day. The term "Relative Humidity" refers to the moisture content in the air "relative" to what the air could hold at that temperature. In contrast "Absolute Humidity," is the absolute amount of water vapor in the air (normally expressed in unit mass of water vapor per unit mass of air).

The moisture-holding capacity of air depends on its temperature. Warmer air can hold more moisture than cooler air. Consequently, relative humidity is highest during the cool morning and evening hours and lowest in the hot afternoon hours. Since inlet air fogging systems cause a very small pressure drop in the inlet air stream, and are relatively inexpensive to install, they have been successfully applied in areas with very high summer time humidity such as the Texas Gulf Coast region or the state of Florida in the USA and in the other high humidity locations in the world. This is because during the hot hours, the coincident relative humidity is typically low.

5 METHODOLOGY AND ANALYSIS TO CREATE AN INTERNATIONAL DATABASE FOR EVAPORATIVE COOLING DEGREE HOURS.

Data was obtained from a climatic database published by Airforce Combat Climatology Center. The goal of the analysis was to determine the Equivalent Cooling Degree Hours (ECDH) for a variety of locations worldwide. The ECDH is defined as a number that provides the total amount of cooling that can be derived for a given time period. The total ECDH is arrived at by summing the ECDHs derived for the 12 months at a location. Results are shown for approximately 106 cities in Table 1 in Appendix A. For example, the total ECDH for Athens, Greece of 29,900 ECDHs is derived by summing the numbers in that row, from January to December.

The database provides a wide range of information including Dry bulb temperature values, and percentage of occurrence, wet bulb temperatures ranges and coincident dry bulb temperatures, and humidity ratios.

After data was collated from the above data files, a cross check was performed with ASHRE data. Finally, the data was placed in a spreadsheet and then a tabulation provided in the Appendix A was derived. The ECDH was chosen with a lower WBT limit of 55°F (12.8°C)[3]. This was considered a very conservative number to avoid any possibility of inlet icing. Figure 7 through 12 show climatic data for New Delhi, India. Similar sets of curves are presented in Figures 13-17 for Berlin, Madrid, Rio de Janeiro, Riyadh, and Sydney. These curves provide a graphic representation of the availability of cooling in different regions of the world.

The number of ECDHs for which certain wet bulb depression ranges are available are shown in Table 2 of Appendix B. The ranges selected are in groups 0-5°C, 5-10C, 10-15°C, 15-20°C, and >20C. Due to rounding issues and temperature recording approaches, the summation of the ECDHs in this table, may differ up to 5% from the Table 1.

[3] Figures 7-12 show the sensitivity of the results to the choice of minimum WBT.

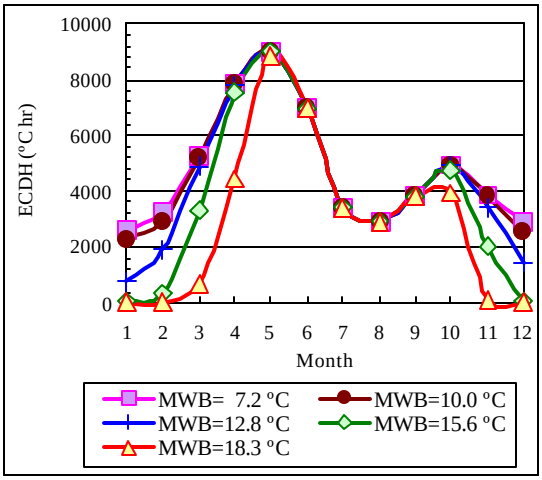

Figure 7. Data for New Delhi, India. This provides the months of the year on the abscissa and the ECDH on the ordinate. The graph provided a month-by-month number of the ECDH, for a range of Minimum Wet Bulb Temperatures ranging from 18.3°C to 7.2°C. The "Bimodal" pattern occurs here because after the hot months of April and May, temperatures drop due to the monsoons and then peak again in the months of September and October.

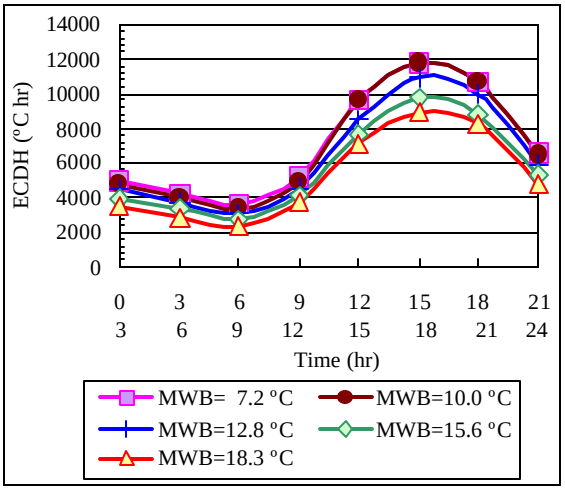

Figure 8. Data for New Delhi, showing the duration of the day that the cooling potential is available. This graph shows that the cooling potential is predominantly clustered between 12:00-21:00 hours. Graphs such as this allow users to match evaporative cooling to peak demand needs.

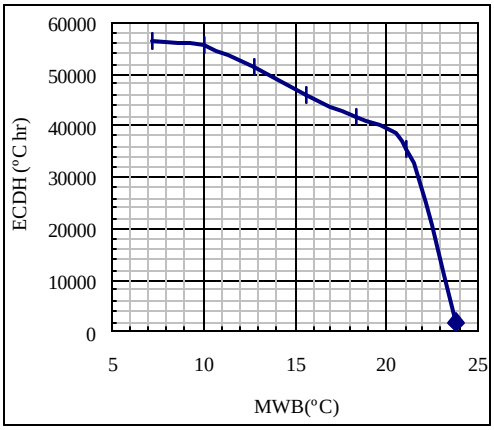

Figure 9. Data for New Delhi showing the sensitivity of ECDH to the minimum wet bulb temperature. For example if the minimum WBT is set to 15°C, then the value of the ECDH is approximately 47,000. If a more aggressive minimum temperature of 10°C is chosen, then the ECDH increase to 56,000.

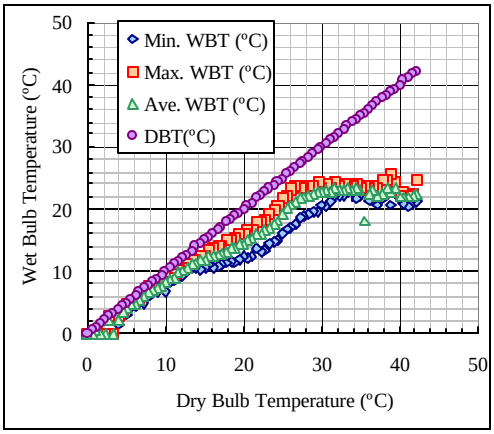

Figure 10. Data for New Delhi, India. This shows the relationship between DBT and WBT. At a temperature approximately 40°C, a wet bulb depression of approximately 20°C is available.

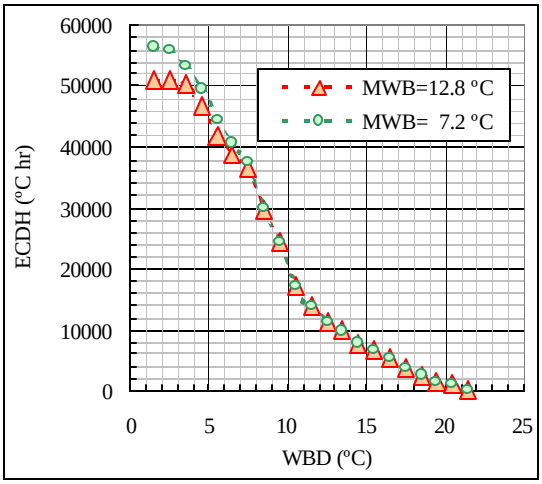

Figure 11. Data for New Delhi, India. ECDH for a variety of wet bulb depressions. For example, at a wet bulb depression of 5°C, and a minimum wet bulb temperature of 7.2°C. At low WBDs the Minimum Wet Bulb Temperature becomes important, as expected.

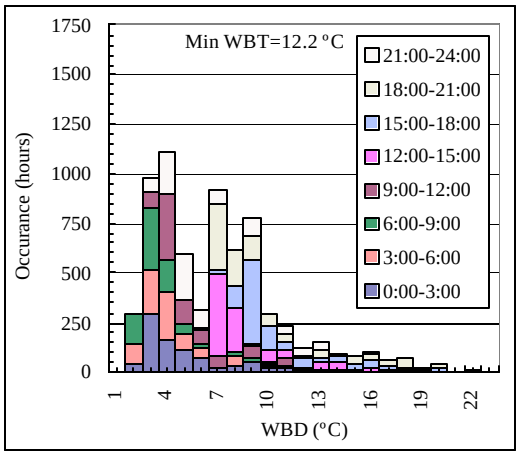

Figure 12. Data for New Delhi, India. Graph showing the time frames during a day when the cooling hour potential exists for a range of wet bulb depressions. At a WBD of 4°C, approx 1125 hours exist and the time distribution of these hours is shown.

5.1 Use of the Equivalent Cooling Degree Hour (ECDH) Table in Appendix A

Any gas turbine operator can immediately see the potential for evaporative cooling per month in his or her location based on a long term historical database by using Table 1 in Appendix A. The results can be directly read off the tabulation providing the total ECDH and it is relatively easy to compute the kW-hours of capacity available by the use of evaporative fogging. In order to do this, the ECDH number would be multiplied by the turbine specific kW/°C cooling number. This can be obtained from the gas turbine OEM's curves. In order to make the task easier, Table 3 in Appendix C provides a detailed tabulation of over 35 gas turbines (both 50 and 60 Hz operation) with runs made to examine the performance sensitivity to changes in ambient conditions. Gas turbines chosen range from 5-250 MW in output and the temperature effects on power are presented in terms of both power boost% per °C and also in terms of MW/ °C. The use of this table will allow users to make an assessment of their gas turbines.

ECDH data can also be looked at more closely to account for differences in energy market values at different times of the year. For example, examination of data could provide an estimate of the revenue stream during the hot summer months alone. An economic evaluation can then be developed on a month-by-month basis knowing the site-specific economic criteria.

5.2 Practical Aspects

If the ECDH number is used to compute MW-hr boost over the year, it is important to note that this would imply that fogging is employed whenever there is even a 1°C depression. In reality there may be a delay set in the control system to trigger the first stage of cooling and also the cooling degrees per stage, would have to be larger than the depression. Typical stage cooling is 1-1.7°C (2-3°F) Further, there is a practical limitation in that in the cooler months, it may be possible that freezing conditions may occur during the early morning and then during the day, an adequate temperature drop may exist. Some operators may drain the skid and hence may not make use of this period of evaporative cooling potential. If power is needed however, then operators may elect to drain during the night and utilize the system during the day. Because of these factors it is impossible to make adjustments in the ECDH tabulation. Users may want to multiply the total number by a factor of 0.97[4] to account for these factors.

5.3 Lowest Temperature for Cooling

Table 1 (Appendix A) has been based on a minimum temperature of 12.8°C (55°F). This is a conservative number in terms of anti icing. Several OEMs publish a combination of relative humidity and temperature at which anti icing measures are turned on. With fogging applications where the ending relative humidity is close to 100%, temperatures as low as 10°C can be utilized[5]. However to be on the very conservative side, temperatures of 12.8°C have been considered.

6 GAS TURBINE SIMULATION

In order to put the entire situation into perspective, a GTPRO simulation was made using a Frame 7121EA and a Frame 9351FA gas turbine in simple cycle configuration (fueled by natural gas) as a reference plant. Salient particulars of this gas turbine are when operating under varying wet bulb depressions of 8 and 12°C from the base temperature are presented in Table 4 (Appendix D)

7. ECONOMIC CRITERIA FOR INLET COOLING

The specific decision to utilize inlet evaporative fogging technology is an economic one and the total project cost must be evaluated over the life cycle. Because of the varying economic situation in different parts of the country, no economic analysis is presented here. Dominating factors which should be taken into account in doing a study are:

- Climatic Profile (discussed above)
- Installed cost of the cooling system in terms of $ /incremental power increase
- Amount of power gained by means of inlet air-cooling. This should take into account parasitic power used, and the effect of increased inlet pressure drop. With fogging systems, the maximum parasitic power is in 50-80 kW for larger turbines when the maximum wet bulb depression has to be derived. The inlet pressure drop is almost nil due to the configuration and design of the nozzle array.
- Fuel and demin water costs, and costs of incremental power- i.e., what benefit is attained by the power boost.
- Projected O&M costs for the system
- Environmental impact
- For cogeneration applications, the time of use electric rates and the power purchase agreement have to be carefully considered
- Potential impact on existing emission licenses

[4] This factor is an estimate, and may go as low as 0.94 in extreme cold locations.

[5] There are several considerations other than just calculating the intake temperature static depression caused by air acceleration to Mach numbers of 0.5 to 0.8. There is also some heating (although small – of the order of 1°C) due to the condensation that occurs and also due to heat transfer from the number 1 bearing etc.

Economic analysis for inlet cooling systems may be found in Utamura et al [11], Ondryas [12], van Der Linden and Searles [13] and Guinn [14].

8. CLOSURE

The paper has provided a tool to easily enable operators in world wide locations to determine the degree of evaporative cooling potential in terms of evaporative cooling degree hours. The analysis and tabulations help users by distilling a huge amount of climatic data into a quick and easy to use format. Any gas turbine operator can use the data to get an idea as to the feasibility of the application of inlet fogging. Further, the data provided would reduce the effort that is needed to make an economic analysis of the potential of evaporative fog cooling.

REFERENCES

.

[1] Chaker, M., Meher-Homji, C.B., Mee T, Nicolson, A., (2001) *"Inlet Fogging of Gas Turbine Engines- Detailed Climatic Analysis of Gas Turbine Evaporative Cooling Potential,"* ASME International Gas Turbine and Aeroengine Conference, New Orleans, USA, June 47, 2001, ASME Paper No. 2001-GT-526. Also to appear in ASME Transactions of Gas Turbine and Power.

[2] McNeilly, D., (2000), *"Application of Evaporative Coolers for Gas Turbine Power Plants,"* ASME Paper No: 2000-GT-303, International Gas Turbine and Aeroengine Congress, Munich, Germany, May 8-11, 2000.

[3] Kitchen, B.J., Ebeling, J.A. (1995), "*QUALIFYING combustion Turbines for Inlet Air Cooling Capacity Enhahcement,"* ASME Paper No: 95-GT-266, International Gas Turbine and Aeroengine Congress, Houston, Texas, June 5-8, 1995.

[4] Tawney, R., Pearson, C., Brown, M, (2001) *"Options to Maximize Power Output for Merchant Plants in Combined Cycle Applications,"* ASME International Gas Turbine and Aeroengine Congress, New Orleans, USA, June 4-7, 2001, ASME Paper No. 2001-GT-0409

[5] Jones and Jacobs (2000) "*Considerations for Combined Cycle Performance Enhancement Options*". GE Publication GER-4200

[6] Johnson, R.S., (1988), "*The Theory and Operation of Evaporative Coolers for Industrial Gas Turbine Installations*," ASME Paper No: 88-GT-41, International Gas Turbine and Aeroengine Congress, Amsterdam, Netherlands, June 5-9, 1988.

[7] Meher-Homji, C.B., and Mee, T.R. (1999) *"Gas Turbine Power Augmentation by Fogging of Inlet Air,"* Proceedings of the 28th Turbomachinery Symposium, Turbomachinery Laboratory, Texas A&M University, September 1999, Houston, Texas.

[8] Meher-Homji, C.B., and Mee, T.R. (2000) *"Inlet Fogging of Gas Turbine Engines- Part A: Theory, Psychrometrics and Fog Generation .and Part B: Practical Considerations, Control and O&M Aspects*," ASME Turbo Expo 2000, Munich May 2000. ASME Paper Nos: 2000-GT-307, 2000-GT-308.

[9] Bhargava, R., Meher-Homji, C.B. (2002*), " Parametric Analysis of Existing Gas Turbines with Inlet Evaporative and Overspray Fogging,"* ASME International Gas Turbine and Aeroengine Conference, Amsterdam, The Netherlands, June 3-6, 2002, ASME Paper No: 2002-GT-30560

[10] Ingistov, S. (2000), *"Fog System Performance in Power Augmentation of Heavy Duty Power Generating Gas Turbines GE Frame 7EA"*. ASME International Gas Turbine and Aeroengine Congress, Munich Germany May 811, 2000, ASME Paper No: 2000-GT-305.

[11] Utamura, M., Ishikawa, A., Nishimura, Y., Ando, N. (1996) *"Economics of Gas Turbine Inlet Air Cooling System for Power Enhancement,"* ASME Paper No: 96-GT-515, International Gas Turbine and Aeroengine Congress, Orlando, Birmingham, UK, June 10-13, 1997.

[12] Ondryas, I.S. *"Options in Gas Turbine Power Augmentation Using Inlet Air Chilling"*, ASME Paper 90-GT-250.

[13] Van Der Linden, S., Searles, D.E., (1996), "*Inlet Conditioning Enhances Performance of Modern Combined Cycle Plants for Cost –Effective Power Generation*," ASME Paper No: 96-GT-298, Intern ational Gas Turbine and Aeroengine Congress, Birmingham, UK, June 10-13, 1996.

[14] Guinn, G.R., (1993), "*Evaluation of Combustion Gas Turbine Inlet Air Precooling for Time Varying Annual Climatic Conditions*," ASME Gogen –Turbo 1993, Bournemouth, UK September 21-23, 1993, IGTI-Volume 8.

Berlin, Germany

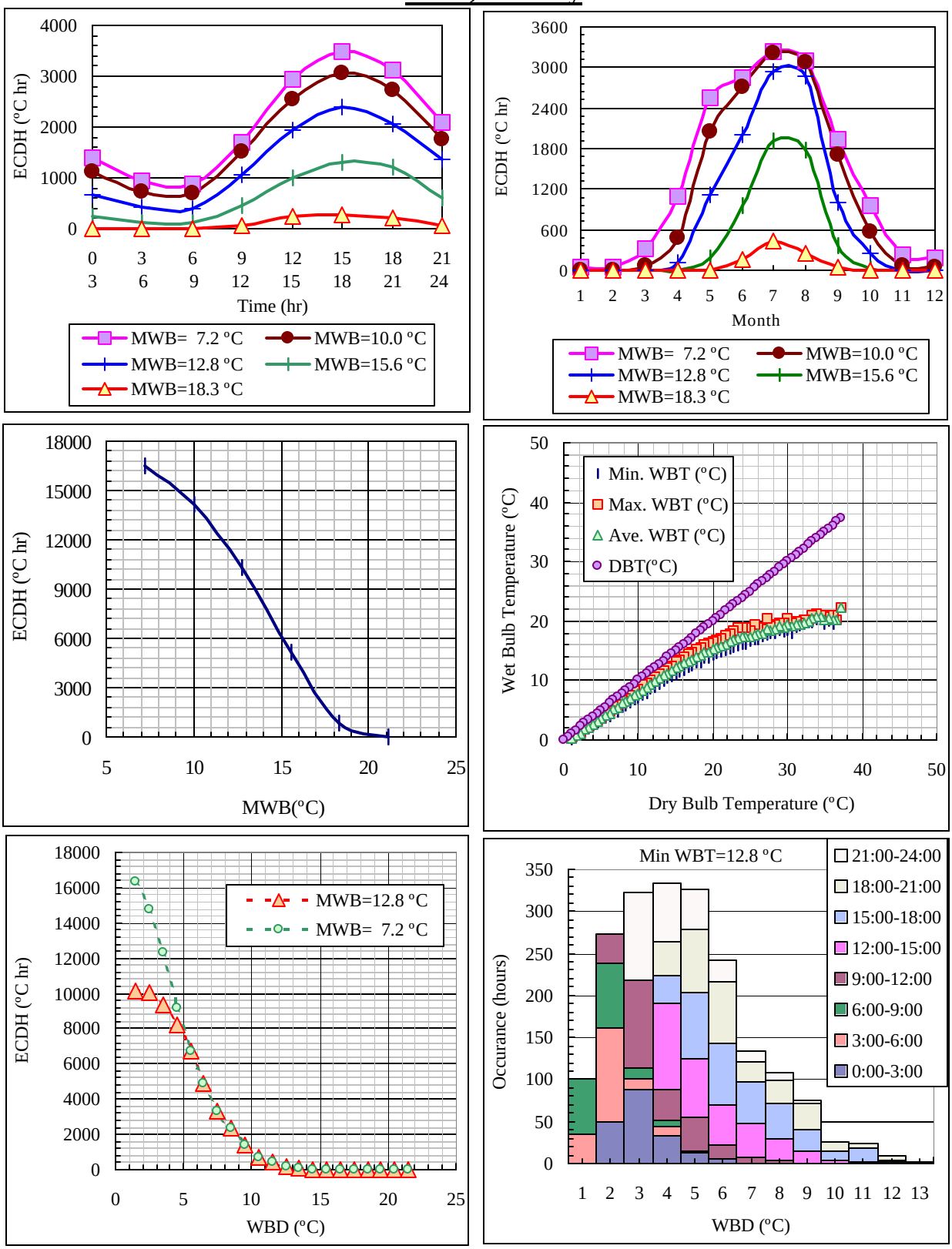

Figure 13. Weather Data Analysis for Berlin, Germany.

Madrid, Spain

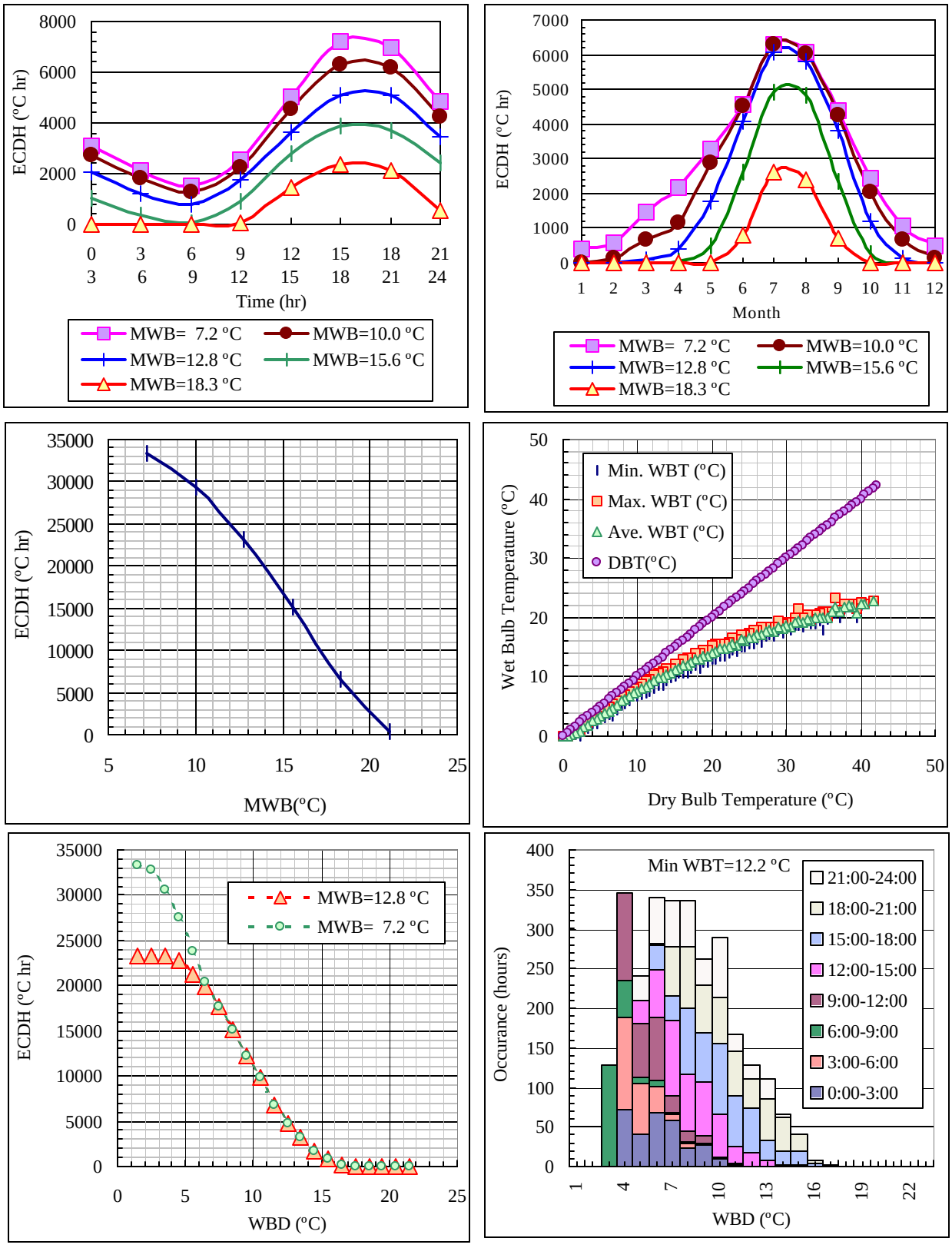

Figure 14. Weather Data Analysis for Madrid, Spain

Rio De Janeiro, Brazil

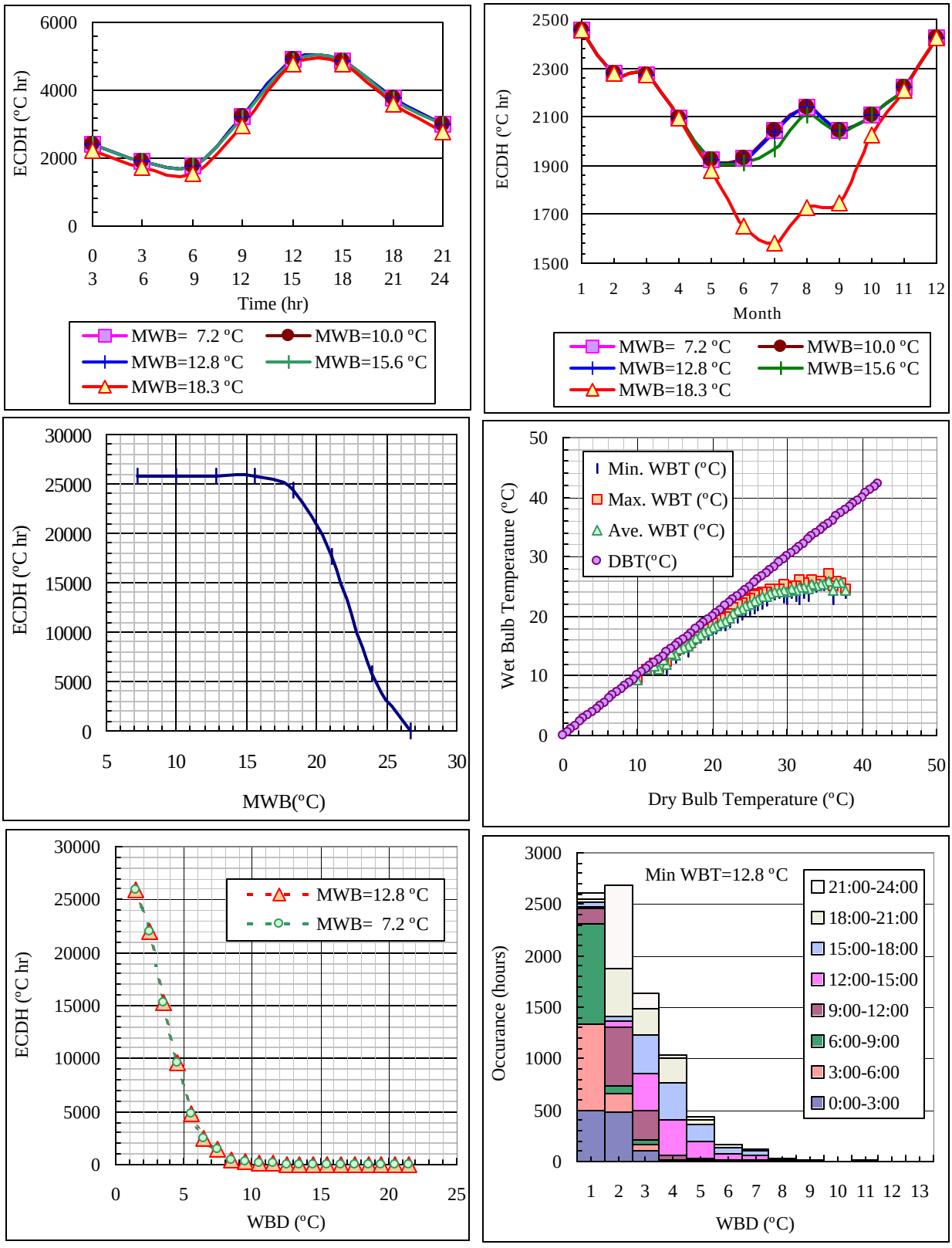

Figure 15. Weather Data Analysis for Rio De Janeiro, Brazil

Riyadh, Saudi Arabia

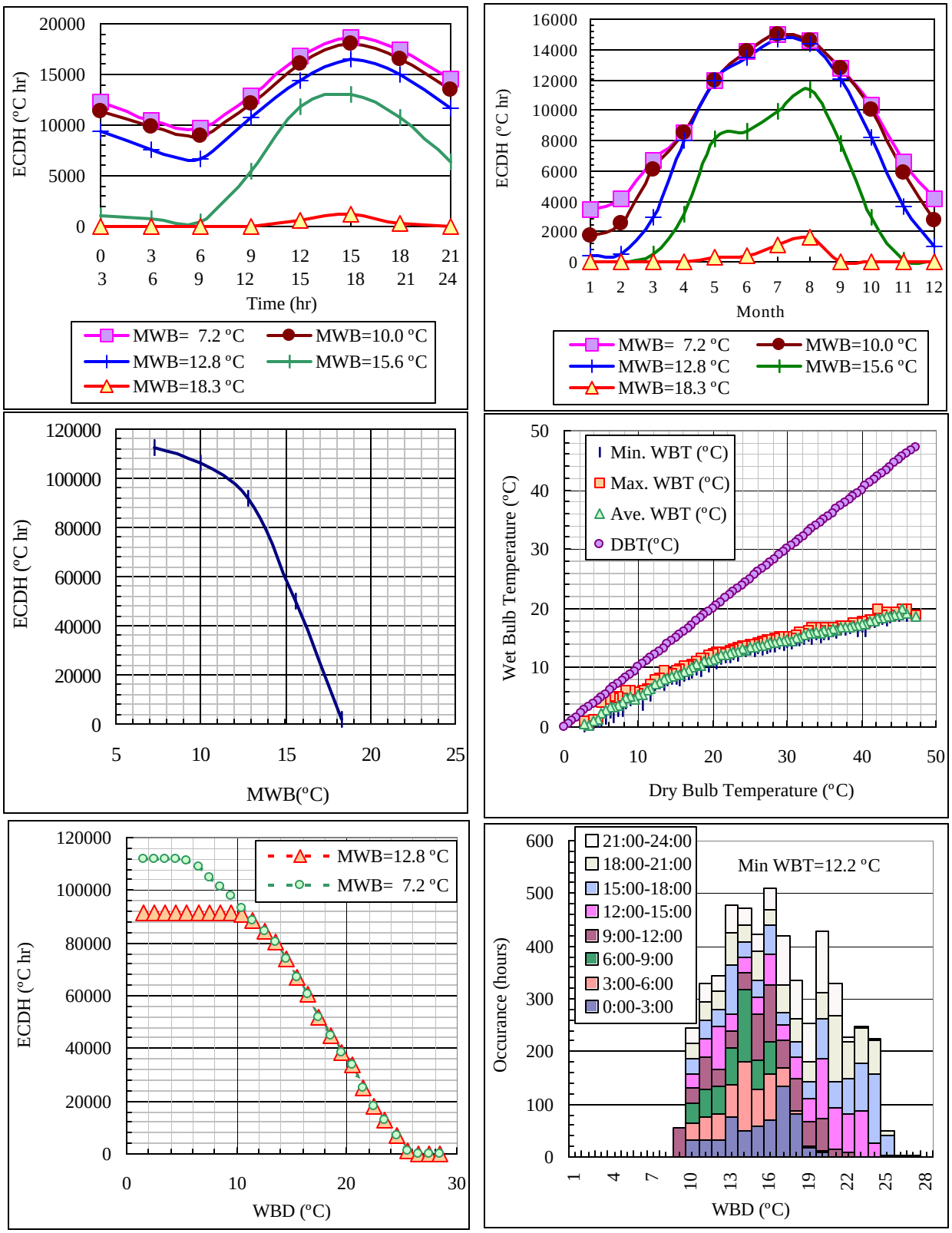

Figure 16. Weather Data Analysis for Riyadh, Saudi Arabia

Sydney, Australia

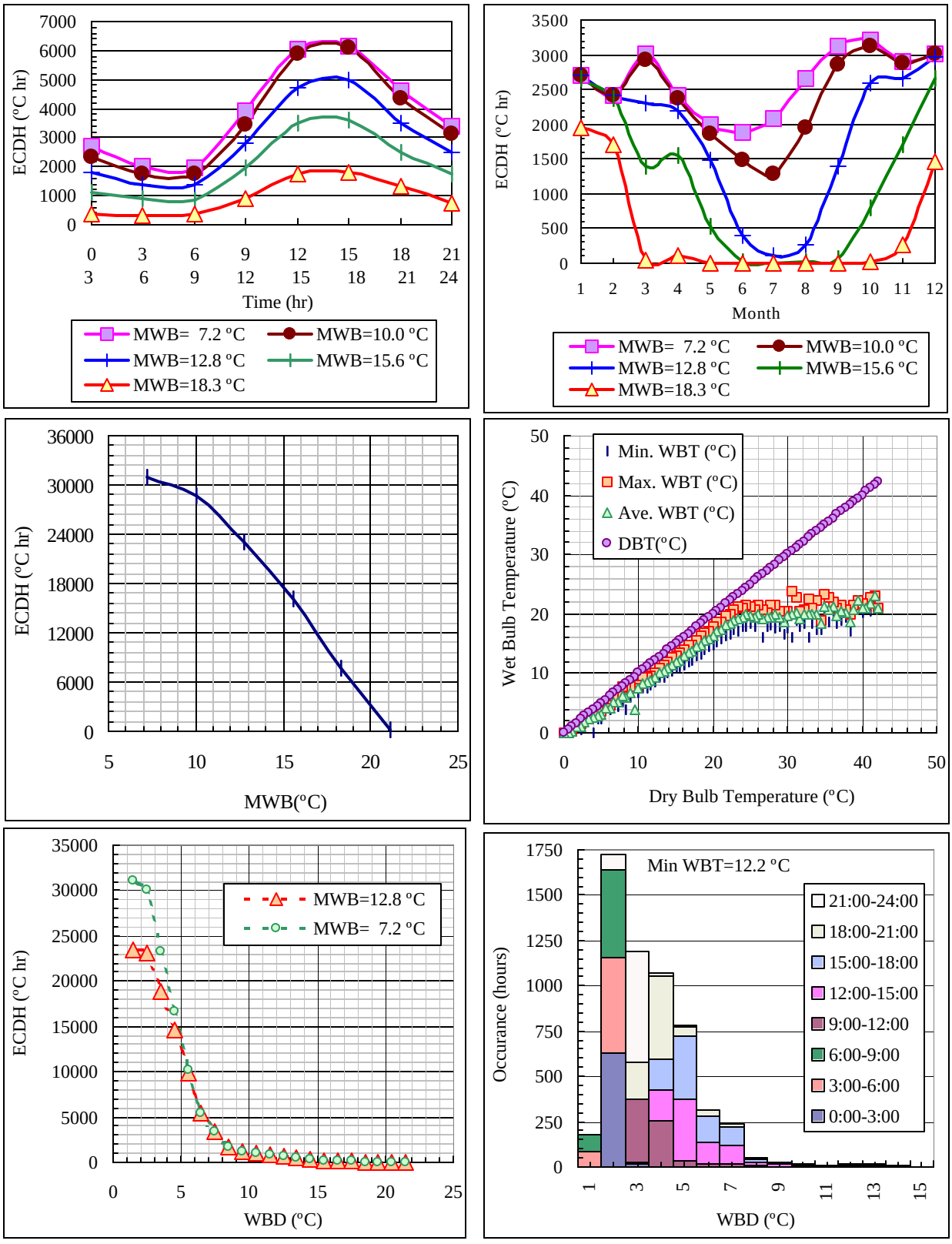

Figure 17. Weather Data Analysis for Sydney, Australia

Appendix A
Available Yearly and Monthly ECDH in 106 cities worldwide
Based on Data From: Air Force Combat Climatology Center (AFCCC)
Min WBT=12.8 °C

	Ann.	Jan.	Feb.	Mar.	Apr.	May	Jun.	Jul.	Aug.	Sep.	Oct.	Nov.	Dec.
Algeria, Dar El Beida	21331	245	367	834	1256	2021	2642	3270	3369	2942	2348	1407	630
Argentina, Buenos Aires	20370	3580	2659	2391	1473	763	274	261	467	894	1759	2540	3309
Australia, Adelaide	23134	4149	4046	3483	2113	887	170	11	86	394	1614	2600	3581
Australia, Melbourne	14004	2837	2729	2316	1178	358	27	4	21	236	758	1390	2151
Australia, Sydney	21490	2699	2419	2314	2200	1489	399	101	268	1391	2590	2661	2961
Austria, Salzburg	9564	0	0	20	85	1047	1878	2579	2416	1272	268	0	0
Bahamas, Nassan	27894	2112	2053	2512	2684	2547	2251	2550	2300	2242	2277	2147	2219
Bermuda, Bermuda	28194	1969	1540	1779	2324	2347	2161	2532	2871	2765	2789	2730	2385
Brazil, Belem	18543	1239	957	1057	1057	1385	1715	1871	1960	1906	1911	1859	1625
Brazil, Rio De Janeiro	29738	2883	2716	2587	2285	2096	2081	2265	2485	2382	2609	2649	2699
Burma, Rangoon	28702	3671	3879	4129	3942	2366	924	863	830	1111	1588	2257	3143
Canada, Halifax	6495	0	0	2	28	336	1413	1904	1752	871	168	20	1
Canada, Kamloops	15242	0	0	0	87	917	2992	4826	4538	1798	83	2	0
Canada, Montreal	10204	0	0	2	132	1121	2343	2797	2377	1154	251	28	0
Canada, Ottawa	10690	0	0	5	181	1107	2508	3043	2509	1080	234	23	0
Canada, Toronto	10699	0	0	20	232	1008	2360	2957	2478	1298	298	45	3
Canada, Vancouver	7496	0	0	0	65	552	1354	2132	2057	1158	172	7	0
Chile, Pudahuel	21158	4072	3361	2955	1580	498	91	44	265	595	1551	2563	3583
China, Beijing	17051	0	0	0	551	3847	4105	2623	2392	2775	758	0	0
China, Hong Kong	26221	1529	1299	1531	1735	1945	2106	2406	2447	2736	3300	3004	2184
China, Shanghai	12894	2	47	109	894	1991	1669	1889	1938	1911	1804	587	54
Colombia, Bogota	8394	729	876	1044	936	968	733	131	156	272	792	847	910
Costa Rica, San Jose	28680	3406	3297	3665	3277	2031	1555	1994	1911	1332	1448	1912	2851
Cuba, Havana	24076	1889	1874	2361	2534	2360	1955	2040	2001	1716	1724	1750	1873
Dominican, Caucedo	21988	1847	1826	2090	2085	1842	1880	1960	1956	1644	1618	1550	1687
Ecuador, Quito	1400	270	270	298	376	44	6	10	2	5	6	9	103
Egypt, Alexandria	27462	602	730	1336	2609	3061	3043	2916	3122	3266	3051	2412	1313
Egypt, Cairo	41696	77	325	2045	4908	6106	5990	5035	4719	4544	4207	2865	876
El Salvador, San Salvador	27213	3209	3200	3304	2922	1943	1490	1718	1546	1294	1625	2204	2757
France, Lyon	12904	0	0	33	216	1326	2213	3306	3295	1841	640	30	5
France, Marseille	18192	0	9	98	296	2158	3251	4212	3909	2635	1321	267	35
France, Paris	10512	0	0	23	181	960	1881	2756	2833	1439	391	47	1
Germany, Berlin	10300	0	0	0	114	1122	2004	2937	2866	1007	249	0	1
Germany, Frankfurt	10392	0	0	7	131	1108	1970	2880	2803	1250	238	4	0
Germany, Munich	8102	0	0	2	29	833	1495	2318	2216	1012	197	0	0
Germany, Stuttgart	8669	0	0	4	42	802	1587	2460	2424	1103	245	2	0
Greece, Athens	29900	64	88	223	1074	3254	4545	6022	6106	4669	2722	849	283
Greece/Crete, Khania	28161	49	55	213	1367	3451	4887	5192	4931	3848	2616	1190	364
Greece, Larissa	25179	5	5	145	752	2767	4746	5670	5176	3761	1845	288	19
Guatemala, Guatemala	25076	2131	2227	2735	2803	2448	1694	1968	1813	1479	1837	1913	2030
Honduras, Tegucigalpa	33254	2652	2979	4016	3971	3252	2408	2643	2643	2266	2075	2045	2304
Hungary, Budapest	13946	0	0	31	206	1779	2670	3493	3443	1901	422	1	0
India, Bombay	37751	4142	4094	4223	3305	3268	2257	1526	1506	1749	3108	4184	4390
India, Calcutta	29665	2596	2963	3959	3275	2757	1913	1549	1460	1555	2272	2726	2641
India, Delhi	51216	751	1900	4897	7806	8976	6984	3423	2898	3791	4931	3397	1462
India, Hyderabad	56761	4329	5193	7353	7841	8251	4465	2841	2431	2785	3577	3706	3987
India, Madras	36921	2485	2497	3030	3066	4177	4704	3928	3645	2899	2279	1937	2276
Iran, Tehran	41226	0	0	0	156	3106	8956	10968	10879	6779	381	1	0
Iraq, Baghdad	66801	41	202	1670	5027	8496	10760	11934	10943	9487	5937	2054	250
Ireland, Dublin	3730	0	0	0	11	125	662	1233	1077	486	117	19	1
Israel, Tel Aviv	26449.16	325	434	1436	2708	2689	2679	2846	3125	3272	3280	2659	997

Table 1. Equivalent Cooling Degree Hours (ECDH)- Degree °C hr for selected cities.

	Ann.	Jan.	Feb.	Mar.	Apr.	May	Jun.	Jul.	Aug.	Sep.	Oct.	Nov.	Dec.
Italy, Milano	13495	0	2	48	370	2012	2693	3129	2766	1816	646	14	0
Italy, Naples	15945	24	9	176	728	2167	2513	3050	2941	2185	1535	491	126
Italy, Venezia	12508	0	0	14	313	1869	2285	2802	2665	1785	731	44	1
Ivoiry Cost, Abidjan	16925	1692	1372	1565	1646	1578	1325	1099	906	948	1338	1694	1763
Jamaica, Kingston	35775	3033	2716	3089	3064	3062	3179	3437	3070	2704	2673	2677	3072
Japan, Fukuoka	16111	13	35	95	1120	2367	2190	2352	2856	2386	2098	555	43
Japan, Nagasaki	15405	15	32	108	1058	2106	1864	2054	2675	2443	2292	700	59
Japan, Osaka	18271	0	7	38	999	2681	2817	2897	3389	2811	2082	533	16
Japan, Tokyo	17307	7	14	40	965	2636	2446	2688	3062	2769	2266	389	23
Jordan, Amman	32838	3	8	122	964	3873	5931	6199	5980	5408	4001	329	19
Korea, Inchon	10895	0	0	0	153	1594	2050	1741	2062	2191	1058	46	0
Korea, Pusan	12494	0	8	8	585	2025	1815	1507	2041	2265	1922	307	10
Korea, Seoul	13518	0	0	0	439	2346	2684	2041	2329	2400	1234	45	0
Lebanon, Beirut	26717	278	476	1236	2397	2623	2815	3062	3076	3608	3552	2608	988
Libya, Tripoli	35984	244	620	1710	3030	4602	4993	5087	4954	4274	3582	2103	786
Malaysia, Kuala Lumpur	21914	1979	1913	1967	1659	1750	1912	1971	2131	1809	1686	1434	1703
Mexico, Mexico	18768	5	2	316	975	3287	3450	2693	2699	2498	2038	804	0
Morocco, Rabat	17497	500	681	1060	1351	1831	1892	2125	2137	2009	1783	1378	750
Netherlands, Amsterdam	6104	0	0	4	93	686	1110	1565	1675	759	201	9	0
Netherlands, H. V. Holland	5702	0	1	18	99	641	827	1382	1566	866	293	10	0
Netherlands, Soesterberg	7321	0	0	5	82	703	1277	2026	2074	915	233	6	0
Netherlands, Volkel	7672	0	0	5	130	830	1447	2050	2037	929	238	5	0
New zealand, Wellington	7288	1602	1384	1225	646	227	39	1	1	61	227	534	1341
Nicaragua, Managua	33984	3351	3571	4307	4382	3372	1974	2110	2220	1916	1766	2156	2858
Norway, Oslo	6328	0	0	0	11	333	1300	2482	2035	165	1	0	0
Pakistan, Karachi	44726	2707	3742	4785	4381	3885	3359	2748	2530	2976	5167	4792	3652
Panama, Tocumen	23012	2653	2773	3225	2777	1730	1320	1466	1466	1231	1166	1275	1931
Paraguay, Asuncion	33315	3506	2837	2995	2315	1854	1684	2139	2750	3013	3319	3409	3495
Peru, Lima	18664	1924	1736	1862	1505	1369	1351	1375	1328	1290	1492	1598	1834
Philippines, Manila	28836	2462	2567	3251	3378	3096	2295	2008	1860	1729	1908	2063	2219
Poland, Warsaw	8308	0	0	0	176	1130	1761	2167	2140	761	173	0	0
Portugal, Lisbon	19127	110	151	549	992	1855	2744	3542	3543	2990	1745	661	244
Puerto Rico, San Juan	30917	2567	2495	2983	2884	2624	2560	2560	2594	2402	2434	2314	2501
Russia, Moscow	6550	0	0	0	20	894	1657	2021	1505	448	4	0	0
Saudia Arabia, Dhahran	63262	1215	1756	3387	5398	7953	9430	9416	8466	6258	4823	3261	1899
Saudia Arabia, Riyadh	91256	412	543	2973	7999	11921	13428	14664	14426	12060	8183	3635	1013
Singapore, Singapore	17313	1595	1498	1708	1402	1439	1485	1546	1632	1377	1428	1040	1162
Spain, Barcelona	12546	4	28	80	485	1361	1933	2391	2337	2015	1365	485	62
Spain, Cordoba	29448	27	167	796	1433	2870	4147	5847	6085	4618	2457	782	218
Spain, Madrid	23415	0	1	111	380	1779	4087	6088	5823	3804	1211	129	3
Spain, Sevilla	31874	87	343	1127	1901	3404	4435	5879	5650	4539	2842	1239	428
Sweden, Stockholm	5871	0	0	0	22	394	1189	2269	1786	200	10	0	0
Switzerland, Geneva	10661	0	0	4	18	867	2001	3107	2930	1430	303	2	0
Taiwan, Taipei	20945	1031	902	1204	1579	1737	2006	2637	2511	2236	2049	1670	1384
Thailand, Bangkok	35935	3574	3103	3314	3347	2939	2770	2813	2768	2301	2425	2971	3611
Tunisia, Tunis	24166	222	283	721	1348	2687	3508	4216	3998	3078	2240	1324	541
Turkey, Ankara	15526	0	0	0	105	970	2634	4494	4691	2251	380	0	0
Turkey, Istanbul	16220	0	0	13	364	1776	2995	3413	3270	2696	1402	290	0
Turkey, Izmir	28045	32	69	313	1507	3325	4789	5647	5219	3912	2240	781	211
UK, Edinburgh	3196	0	0	0	15	83	494	1103	1073	340	86	2	0
UK, London Heathrow	8568	0	0	4	82	544	1553	2419	2409	1176	329	51	1
UK, London Gatwick	6755	0	0	2	42	428	1190	1979	1946	901	234	32	0
Uruguay, Carrasco	16244	2739	2093	2039	1313	661	261	247	448	722	1340	1861	2520
Vietnam, Ho Chi Minh	29772	3189	3142	3512	3172	2637	1951	1895	1903	1775	1750	2146	2702
Yugoslavia, Belgrade	14885	0	9	135	538	2082	2422	3118	3289	2324	897	66	6

Table 1. (Cont.) Equivalent Cooling Degree Hours (ECDH)- Degree °C hr for selected cities.

APPENDIX B

Table 2. Availability of ECDH of a Range of WBD (°C)

Min WBT=12.8 °C

	WBD						WBD				
Country, City	0-5.	5-10.	10-15.	15-20.	> 20.	Country, City	0-5.	5-10.	10-15.	15-20.	> 20.
Algeria, Dar El Beida	9666	9934	1382	173	2	Ivory Cost, Abidjan	16704	472	17	5	0
Argentina, Buenos Aires	9021	10422	1019	5	0	Jamaica, Kingston	21025	14632	0	0	0
Australia, Adelaide	4630	12048	6138	1373	62	Japan, Fukuoka	10954	4992	43	0	0
Australia, Melbourne	3600	7172	2849	664	36	Japan, Nagasaki	13161	1723	7	0	0
Australia, Sydney	13327	8522	832	176	8	Japan, Osaka	9931	8428	104	0	0
Austria, Salzburg	2939	6522	418	5	0	Japan, Tokyo	11070	6530	49	0	0
Bahamas, Nassan	23427	4260	0	0	0	Jordan, Amman	2345	16153	14609	1654	6
Bermuda, Bermuda	26897	1298	0	0	0	Korea, Inchon	9148	1786	17	0	0
Brazil, Belem	13408	5694	2	0	0	Korea, Pusan	11968	550	0	0	0
Brazil, Rio De Janeiro	15727	11643	1903	17	0	Korea, Seoul	8318	5966	5	0	0
Burma, Rangoon	13757	9962	4907	70	0	Lebanon, Beirut	18019	7648	411	85	11
Canada, Halifax	4051	2101	14	0	0	Libya, Tripoli	8311	16585	8366	3148	105
Canada, Montreal	5203	4701	0	0	0	Malaysia, Kuala Lumpur	12483	10429	19	0	0
Canada, Ottawa	4409	5681	80	0	0	Morocco, Rabat	14595	2255	564	82	6
Canada, Toronto	4550	5417	59	0	0	Netherlands, Amsterdam	4558	1600	55	0	0
Canada, Vancouver	6535	1272	1	0	0	Netherlands, H. V. Holland	5074	772	64	6	0
Chile, Pudahuel	2885	12404	6149	68	0	Netherlands, Soesterberg	3802	3532	197	0	0
China, Beijing	6005	10907	1207	54	0	Netherlands, Volkel	4268	3361	197	0	0
China, Hong Kong	23809	2082	0	0	0	New Zealand, Wellington	6561	443	0	0	0
China, Shanghai	10938	1906	8	0	0	Nicaragua, Managua	13228	17250	3112	0	0
Costa Rica, San Jose	15063	13124	179	5	0	Norway, Oslo	1385	4461	309	0	0
Cuba, Havana	16028	7606	3	0	0	Pakistan, Karachi	13618	25195	5424	594	32
Dominican, Caucedo	18687	2843	0	0	0	Panama, Tocumen	14664	8362	1	0	0
Egypt, Alexandria	14453	12240	380	116	2	Paraguay, Asuncion	15685	15354	1931	29	0
Egypt, Cairo	7919	17423	14216	2411	159	Peru, Lima	17158	1069	0	0	0
El Salvador, San Salvador	13195	12808	808	0	0	Philippines, Manila	20330	8247	13	0	0
France, Lyon	5155	6414	1085	40	0	Poland, Warsaw	4030	4103	102	0	0
France, Marseille	8234	9460	506	6	0	Portugal, Lisbon	9572	8067	1943	113	0
France, Paris	4874	5370	437	0	0	Puerto Rico, San Juan	20502	10015	8	0	0
Germany, Berlin	3521	5987	708	10	0	Russia, Moscow	3038	3780	57	0	0
Germany, Frankfurt	3872	5830	869	3	0	Saudia Arabia, Dhahran	7821	21525	18775	12128	2920
Germany, Munich	2856	5033	269	2	0	Saudia Arabia, Riyadh	0	1804	25904	32322	32566
Germany, Stuttgart	3040	5164	412	2	0	Singapore, Singapore	14181	4068	0	0	0
Greece, Athens	6647	18772	4262	203	0	Spain, Barcelona	11156	1534	8	0	0
Greece/Crete, Khania	8732	15144	4039	519	8	Spain, Cordoba	5920	13155	7324	2678	12
Greece, Larissa	5569	12259	7481	846	52	Spain, Madrid	1989	11307	8956	807	0
Guatemala, Guatemala	12214	12540	524	2	0	Spain, Sevilla	7039	14087	8566	2040	4
Honduras, Tegucigalpa	12965	17437	2413	7	0	Sweden, Stockholm	2066	3783	125	0	0
Hungary, Budapest	4152	8815	971	0	0	Switzerland, Geneva	3130	6738	621	0	0
India, Bombay	18844	16982	1727	87	6	Taiwan, Taipei	16937	3916	8	0	0
India, Calcutta	13033	15425	1048	114	0	Thailand, Bangkok	15991	18972	568	0	0
India, Delhi	9218	24740	10229	5458	1139	Tunisia, Tunis	10683	11107	1808	160	29
India, Hyderabad	12782	23898	12841	6964	110	Turkey, Ankara	695	7366	6648	594	2
India, Madras	14881	17874	3495	205	0	Turkey, Istanbul	7732	8276	296	6	0
Iran, Tehran	0	617	19861	19726	3789	Turkey, Izmir	6887	14857	5659	159	0
Iraq, Baghdad	22	12781	23710	18502	12200	UK, Edinburgh	2517	656	6	0	0
Ireland, Dublin	3467	219	0	0	0	UK, London Heathrow	4329	3888	258	0	0
Israel, Tel Aviv	16443	9579	423	197	3	UK, London Gatwick	3778	2861	151	0	0
Italy, Milano	6267	7226	34	2	0	Uruguay, Carrasco	12239	3727	335	0	0
Italy, Naples	8304	7485	286	2	0	Vietnam, Ho Chi Minh	15677	13359	219	0	0
Italy, Venezia	8209	4431	4	0	0	Yugoslavia, Belgrade	5552	8397	960	34	0

Appendix C Table 3. Power Boost of Various Gas Turbines.

plant Criteria:

DBT =32 °C **R.H.=50%** **WBT=24 °C**

Nomenclature: **NF**: **N**o **F**og
EC: **E**vaporative **C**ooling
NP:**N**et **P**ower

Id	Gas Turbine	NP (NF) (MW)	NP (EC) (MW)	PB (%)	PB/°C	KW/°C
24	ABB GT 8	40.78	43.39	6.40	0.77	314.5
152	ABB GT 8C2	49.46	52.05	5.24	0.63	312.0
25	ABB GT 11N	69.86	73.78	5.61	0.68	472.3
110	ABB GT 11N2	97.24	103.35	6.28	0.76	736.1
41	ABB GT 13D2	86.77	91.82	5.82	0.70	608.4
70	ABB GT 13E2	139.00	147.51	6.12	0.74	1025.3
18	Aln 501KB5	3.02	3.25	7.62	0.92	27.7
21	Aln 571KA	4.44	4.81	8.33	1.00	44.6
129	Asig ASE40	2.62	2.77	5.73	0.69	18.1
151	Asig ASE50A	2.99	3.25	8.70	1.05	31.3
48	EGT Typhoon	3.24	3.63	12.04	1.45	47.0
145	EGT Typhoon	4.37	4.66	6.64	0.80	34.9
33	EGT Tornado	5.23	5.58	6.69	0.81	42.2
1	GE 5371 PA	22.15	23.86	7.72	0.93	206.0
133	GE 6561 B	34.29	36.42	6.21	0.75	256.6
135	GE 7241 FA	148.58	158.67	6.79	0.82	1215.7
174	GE 9351 FA	227.48	242.08	6.42	0.77	1758.8
113	GE 9391 G	246.85	258.54	4.74	0.57	1408.4

Id	Gas Turbine	NP (NF) (MW)	NP (EC) (MW)	PB (%)	PB/°C	KW/°C
159	GE LM2500PE	18.79	19.88	5.80	0.70	131.3
118	GE LM6000PC	32.25	36.48	13.12	1.58	509.6
161	GE LM6000SPT	33.83	36.19	6.98	0.84	284.3
101	KWU V64.3A	60.04	63.19	5.25	0.63	379.5
43	KWU V94.2	125.96	133.46	5.95	0.72	903.6
154	Mtsb 701 F	228.76	241.82	5.71	0.69	1573.5
169	P+W ST6L-813	0.65	0.71	9.61	1.16	7.5
137	Sol Taurus	4.20	4.52	7.62	0.92	38.6
132	Sol Saturn	0.97	1.05	8.25	0.99	9.6
188	Sol Centaur	3.82	4.10	7.33	0.88	33.7
97	Sol Mars	9.12	9.74	6.80	0.82	74.7
189	Sol Titan	11.17	12.05	7.88	0.95	106.0
44	TP+M FT8	21.03	22.69	7.89	0.95	200.0
13	TP+M FT4C	24.21	26.48	9.38	1.13	273.5
47	W251 B12	39.94	42.89	7.39	0.89	355.4
77	W501 D5A	103.86	110.49	6.38	0.77	798.8
74	W701 F	197.08	209.30	6.20	0.75	1472.3

Appendix D: Table 4: Simulation Run Two Heavy Duty Gas Turbines With Inlet Fogging.

Tamb= 40°C Base case, Fuel is CH4 supplied at 25°C, No fuel compressor.

Fuel LHV 50047 kJ/kg; Inlet / Outlet DeltaP = 10 /12.5 mbar

	FRAME 7111EA (60 Hz)			FRAME 9351FA (50 Hz)		
GAS TURBINE PARAMETER	**BASE CASE Tamb = 40°C**	**WBD = 8°C**	**WBD = 12°C**	**BASE CASE Tamb = 40°C**	**WBD = 8°C**	**WBD = 12°C**
GT gross power [kW]	71,296	75,914	78,158	212,940	228,082	235,519
GT eff [%]	28.48	28.9	29.15	31.72	32.35	32.68
GT gross heat rate [kJ/kWh]	11,391	11,226	11,131	10,229	10,030	9,927
Fog Status	OFF	ON	ON	OFF	ON	ON
Compressor Pressure Ratio	11.2:1	11.6:1	11.9:1	13.1:1	13.6:1	13.8:1
Turbine Inlet Temperature [°C]	1104	1105	1107	1312	1313	1317
Exhaust Gas Temperature [°C]	554	549	546619	619	613	610
Compressor Inlet Mass flow rate [kg/sec]	260	269	274	575	594	606
Ambient Temperature [°C]	40	40	40	40	40	40
Compressor Inlet Temperature [°C]	40	32	28	40	32	28
Compressor Discharge Temperature [°C]	383	376	373	396	384	381
Compressor Disch. Pressure [Bar]	11.28	11.68	11.91	13.13	13.5	13.86
Fuel Flow Rate [Kg/sec]	4.5086	4.7299	4.828	12.089	12.6969	12.976
Axial Compressor Work [kW]	93,754	97,074	99,002	213,701	218,972	222,221
Turbine Section Work [kW]	166,895	174,885	197,084	431,281	451,889	462,675
Fog Water Flow, kg/sec	-	0.907	1.374	-	2.012	3.036